Affinity Capturing and Surface Enrichment of a Membrane Protein Embedded in a Continuous Supported Lipid Bilayer

Anders Gunnarsson+,*[a] Lisa Simonsson Nyström+,[b] Sabina Burazerovic,[b] Jenny Gunnarsson,[a] Arjan Snijder,[a] Stefan Geschwindner,[a] and Fredrik Höök*[b]

Investigations of ligand-binding kinetics to membrane proteins are hampered by their poor stability and low expression levels, which often translates into sensitivity-related limitations impaired by low signal-to-noise ratios. Inspired by affinity capturing of water-soluble proteins, which utilizes water as the mobile phase, we demonstrate affinity capturing and local enrichment of membrane proteins by using a fluid lipid bilayer as the mobile phase. Specific membrane-protein capturing and enrichment in a microfluidic channel was accomplished by immobilizing a synthesized trivalent nitrilotriacetic acid (tris-NTA)–biotin conjugate. A polymer-supported lipid bilayer containing His$_6$-tagged β-secretase (BACE) was subsequently laterally moved over the capture region by using a hydrodynamic flow. Specific enrichment of His$_6$–BACE in the Ni^{2+}–NTA-modified region of the substrate resulted in a stationary three-fold increase in surface coverage, and an accompanied increase in ligand-binding response.

With more than 60% of today's drugs being targeted against membrane proteins, means to investigate their interactions with ligands and drug candidates have become an essential component in contemporary drug development.[1] However, biophysical studies using purified membrane proteins are hampered by low expression levels and poor protein stability. The latter problem originates from the necessity to solubilize the membrane proteins in detergents (or other amphiphiles)[2] to shield their hydrophobic parts from the aqueous environment. However, owing to their low intrinsic stability, this treatment is often associated with loss of protein function. Retained stability and function may be obtained by reconstitution of the puri-

fied membrane proteins back into a lipid environment, utilizing so called proteoliposomes, that is, membrane–protein-containing lipid vesicles.[3] However, the generally high lipid-to-protein ratio in proteoliposomes make ligand-binding studies severely compromised, primarily because the concentration of active proteins becomes significantly reduced. This challenge is particularly apparent when surface sensitive techniques, such as surface plasmon resonance (SPR) or total internal reflection fluorescence (TIRF) microscopy, are used to probe ligand–receptor interactions, in which case sensitivity-related limitations impaired by insufficient signal-to-noise ratios are well documented.[4] As schematically illustrated in Figure 1, we demon-
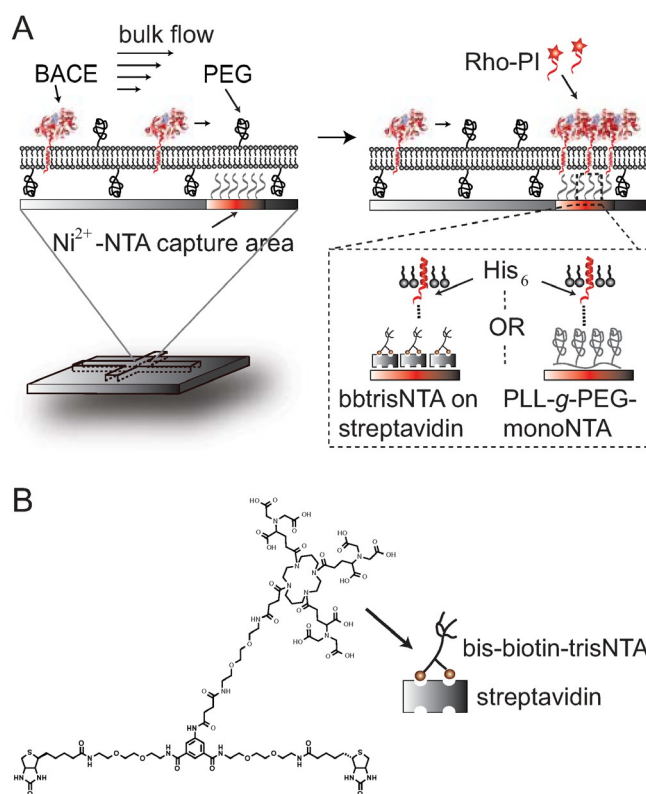

Figure 1. A) Schematic illustration of protein affinity capture in a lipid membrane. Mobile transmembrane BACE with a C-terminal 6×His-tag is laterally moved, by hydrodynamic forces, in the polymer SLB along the microfluidic channel and specifically captured and accumulated at the confined Ni^{2+}-NTA-functionalized surface. Localization of BACE is visualized by addition of a fluorescent peptide inhibitor (Rho-PI). The inset illustrates the two Ni^{2+}-NTA-based surface functionalization strategies employed with tris-(high affinity) versus mono-NTA (low affinity), respectively. B) Chemical structure of bis-biotin-tris-NTA (bbtrisNTA).

[a] Dr. A. Gunnarsson,+ J. Gunnarsson, Dr. A. Snijder, Dr. S. Geschwindner
Discovery Sciences, AstraZeneca R&D Mölndal
43183 Mölndal (Sweden)
anders.gunnarsson@astrazeneca.com

[b] Dr. L. Simonsson Nyström,+ Dr. S. Burazerovic, Prof. Dr. F. Höök
Department of Applied Physics, Chalmers University of Technology
412 96 Göteborg (Sweden)
E-mail: fredrik.hook@chalmers.se

[+] These authors contributed equally

strate in this work how conversion of proteoliposomes into a planar supported lipid bilayer, combined with hydrodynamic manipulation of the membrane proteins over a local capturing region, enables stationary capturing and local membrane–protein enrichment, while embedded in a lipid environment.

The concept presented in Figure 1 was inspired by previous attempts to overcome challenges related to membrane–protein purification and enrichment in the aqueous phase, which was approached for the first time in the early 1990s by using electrophoretic separation and accumulation of mobile components in a laterally fluid-supported lipid bilayer (SLB).[5] Since then, electrophoresis,[6–8] surface acoustic waves,[10] hydrodynamic forces,[11–13] and rectified diffusion[14–16] have been employed for the separation of different membrane constituents maintained in a lipid-bilayer environment. However, so far, separation has been restricted to rapidly diffusing lipids[5,7,11,14–16] and lipid-bound[8,10,12] or GPI-linked[17] proteins, whereas handling and spatial manipulation of transmembrane proteins have been hampered by the difficulty in making SLBs containing mobile membrane proteins. The reduced mobility has primarily been attributed to the narrow gap (1–3 nm) between the bilayer and the solid support,[18] and separation and enrichment of specific membrane proteins embedded in a continuous SLB have, therefore, remained an unsolved challenge.

To demonstrate spatial manipulation and local enrichment of a transmembrane protein, we selected the transmembrane protease, β-secretase 1 (BACE), which contributes to the cleavage of the amyloid precursor protein (APP) into amyloid-β peptides, a process strongly implicated in the pathogenesis of Alzheimer's disease.[19] To ensure high mobility of BACE in the SLB, that is, to make it possible for the lipid bilayer to function as the mobile phase for affinity capturing, a polymer-supported BACE-containing SLB was formed through the co-adsorption of proteoliposomes containing reconstituted BACE and PEGylated POPC liposomes (0.5 wt% PEG5000-Ceramide) at a 1:1 ratio on the glass floor of a microfluidic channel (see the Supporting Information for details). The presence of a small fraction (< 0.1%) of NBD-labeled liposomes enabled the in situ visualization of SLB formation during each experiment (Figure 2A).

The presence of mobile BACE with a diffusivity of 0.17 ± 0.02 $\mu m^2 s^{-1}$ and a mobile fraction of approximately 70% with (and 0.19 ± 0.02 $\mu m^2 s^{-1}$ and ca. 50% without) PEG-lipids in the SLB (Figure 2B) was confirmed by using fluorescence recovery after photobleaching (FRAP) measurements after addition of a rhodamine-labeled peptide inhibitor (Rho-PI), known to bind specifically to the catalytic site of BACE[20] protruding into the bulk solution. No unspecific binding to the membrane was observed in the absence of BACE (Figure S2C). The diffusivity of BACE was approximately ten times slower than that of a typical lipid, which is in good agreement with previous reports for proteins that span the membrane with a single transmembrane helix.[21] The increased mobile fraction observed for BACE in the PEGylated compared with non-PEGylated SLBs suggests that unfavorable interactions between the membrane protein and the underlying substrate were reduced by the use of PEG in the SLB.[22]
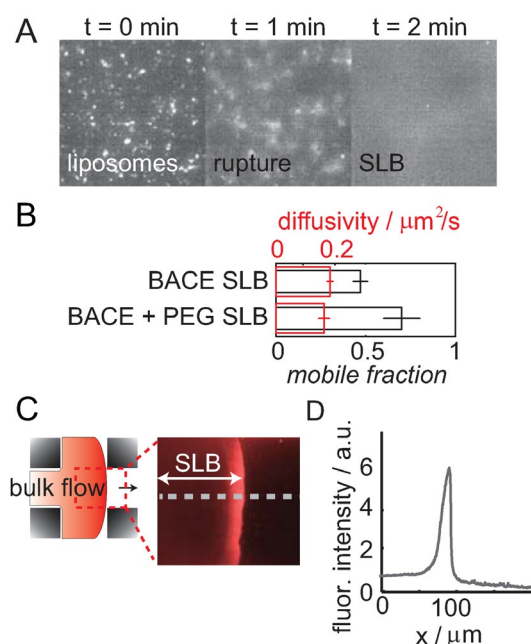

Figure 2. A) Fluorescence micrograph snapshots (70×70 µm²) of liposome adsorption, rupture, and fusion leading to SLB formation visualized by including a small fraction (< 0.1%) of NDB-labeled liposomes. B) Extracted diffusion coefficients and mobile fractions of BACE in the absence and presence of PEG. C) Fluorescence micrograph (190×150 µm²) of BACE-containing polymer SLB after exposure to a flow of 200 µL min⁻¹ for 15 min in the microfluidic chip. BACE accumulation at the front on the SLB is visualized by injection of a fluorescently labelled peptide inhibitor. D) Intensity profile across the channel, corresponding to the white dotted line.

In analogy with previous reports on hydrodynamic enrichment at the front of the lipid bilayer of DNA,[23] lipids,[11] and lipid-bound proteins,[12] the mobile fraction of BACE with the active site pointing away from the surface could be successfully accumulated at a bilayer front by applying a hydrodynamic shear force in the microfluidic channel (see Figures 2C and 2D as well as the Supporting Information). By using a fluorescent peptide inhibitor that binds to the active site of BACE to indirectly label the protein, it prevents investigation of the fraction of BACE pointing towards the surface.

The intensity line profile revealed that the protein enrichment resulted in a six-fold increase in the coverage of BACE (Figure 2D). However, protein enrichment at the front of a SLB is subject to diffusional broadening and rapidly relaxes as soon as the shear flow is interrupted. Moreover, accumulation at a bilayer front is not selective for a specific protein. Hence, this concept alone is not sufficient to overcome the surface coverage-related sensitivity limitations encountered for surface-based sensors applied to study temporally resolved ligand binding to transmembrane proteins.

To also accomplish that goal, we speculated that 1) the solid support underneath the SLB could be chemically modified to enable selective and local capture of the membrane protein of interest, with the imperative that 2) the lipid membrane could freely pass over the capturing region; the latter being fulfilled by the PEG cushion lifting the SLB over the substrate[24] (Figure 1A).

Free passage of a PEGylated SLB over a chemically modified capturing area was explored and optimized by using hydrodynamic forces to laterally move the SLB from a clean SiO_2 region to a chemically modified area located on the same substrate. This approach was used to exploit the fact that SLB formation readily occurs on clean SiO_2, thereby avoiding SLB formation directly onto a chemically modified surface, which is known to be inefficient because of the strong adhesion strength between the vesicles and the substrate required for SLB formation to occur spontaneously.[25]

The micrographs in Figure 3 A illustrate a representative experiment, starting with flow-controlled deposition of (BACE-free but fluorescently [1 wt %] labeled) liposomes, which were spontaneously converted into an SLB in the left half of the cross-channel geometry, before subsequent surface functionalization, restricted to the right half of the channel. By increasing the flow speed from the left (while interrupting the flow from the right), the hydrodynamic force acting on the PEG-supported membrane induced a lateral movement of the SLB towards the area of the chip functionalized with fluorescently labeled streptavidin (streptA-FITC) or PLL-g-PEG-rhodamine.[26]

Intensity profiles confirmed that the adsorbed polymer was not removed by the moving SLB front (Figure 3 B). Fluorescence resonance energy transfer (FRET) between streptA-FITC

and rhodamine-PE lipids prevented the corresponding quantification when streptavidin constituted the functionalized area. However, the intensity profiles suggest that a significant amount (>25 % of the original intensity) of streptA-FITC remained bound after passage of the SLB front (Figure S7). More importantly, the presence of PEG-lipids in the SLB was a prerequisite for lateral movement *onto* both types of surface modifications. The motion of a pure POPC SLB was completely hindered at the edge of the surface modification, while it extended over the surface-modified regions when PEG-lipids were included in the SLB (Figure 3 B). By moving the SLB across a "ladder" of increasing coverage of PLL-g-PEG (Figure S4) or streptavidin, the mobility of PEGylated SLBs was not hindered, even at saturated binding of streptA-FITC to SiO_2 (corresponding to ca. 25 % of full protein coverage on a planar surface, see Figure S7), whereas the motion became hampered above 25 % surface coverage of PLL-g-PEG (Figure S4). Furthermore, FRAP measurements of the SLB on bare SiO_2 and on the functionalized area (positions 1 and 2 in micrographs in Figure 3 A) showed insignificant differences in diffusivity (Figure 3 C), suggesting that the SLB extends as a homogeneous and continuous film on top of the surface functionalized areas.

These experiments, which established the conditions for the motion of PEGylated (protein free) SLBs over surface-adsorbed streptavidin and PLL-g-PEG, were inspired by the fact that both surface modifications can be used to introduce a NTA-Ni^{2+} functionality for selective capture of His-tag engineered proteins, as previously shown for water-soluble or solubilized proteins.[27,28] To explore if a His_6-tagged membrane-residing protein could also be captured, a BACE-containing PEGylated SLB was moved over an NTA-Ni^{2+}-functionalized stripe located in the center of the microfluidic channel (Figure 4 A).

As detailed above (Figure 2), a proteoliposome mixture was first added to form the BACE-containing PEGylated SLB in the left SiO_2-exposed part of the chip (left panel in Figure 4 A) without initially overlapping with the NTA-Ni^{2+} stripe. This was subsequently followed by formation of a pure PEG-SLB, that is, without BACE, over both the NTA-Ni^{2+} stripe and the right (SiO_2-exposed) part of the chip (middle panel in Figure 4 A). Note that, even when liposome rupture over the functionalized surface area (in contrast to surrounding SiO_2) was not complete, the hydrodynamic force-controlled motion of the SLB (right panel in Figure 4 A) induced additional rupture and facilitated the formation of a continuous SLB.[13]

As the monovalent NTA modification of PLL-g-PEG is known to display relatively low affinity ($K_d \approx$ μM) towards His_6-tagged proteins,[29] a heterobifunctional ligand with three NTA moieties, tris-NTA,[30] was synthesized (bbtrisNTA-Ni^{2+}, see the Supporting Information for details). The tris-NTA chelating head combined with a biotinylated anchor ensures higher affinity ($K_d \approx$ low nM) towards the His_6-tag[30] and firm binding to streptavidin. The hetero-bifunctionality of bbtrisNTA-Ni^{2+} was confirmed by utilizing SLB-containing BACE molecules with the His_6-tag protruding towards the bulk. Upon addition of the conjugate, significant binding of streptA-FITC was observed, but protein binding was negligible in the absence of the conjugate (Figure S3).
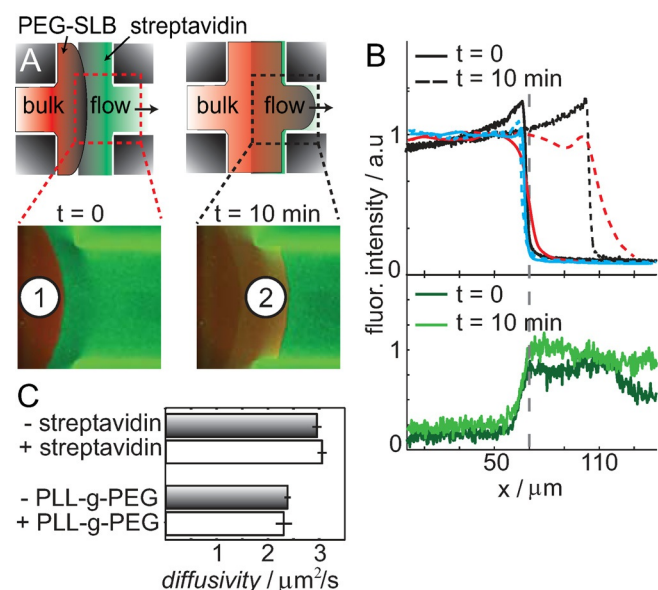

Figure 3. A) Fluorescence micrographs snapshots (190×190 um²) of hydrodynamic force-induced movement of rhodamine-labeled PEG-SLB onto an adsorbed streptavidin–FITC layer. B) Upper panel shows intensity profiles through the center of the microfluidic channel for the PEG-SLB prior to SLB movement (t = 0, solid lines) and after 10 min of hydrodynamic force-induced movement (dashed line) as it stretches over the adsorbed layer of streptavidin (black) or PLL-g-PEG (red). Intensity profiles corresponding to a POPC SLB lacking the PEG-support are also shown (blue). Lower panel shows corresponding intensity profiles for an adsorbed PLL-g-PEG layer prior to (t = 0) and while (t = 10 min) the PEG-SLB stretches over it. Grey dashed line indicates the position of the SLB and polymer/protein edge prior to exposure of buffer flow. C) Diffusion coefficients of fluorescently labeled lipids (rhodamine-PE or NBD-PE) in the PEG-SLBs on bare SiO_2 (grey bars) and on streptavidin or PLL-g-PEG (white bars).
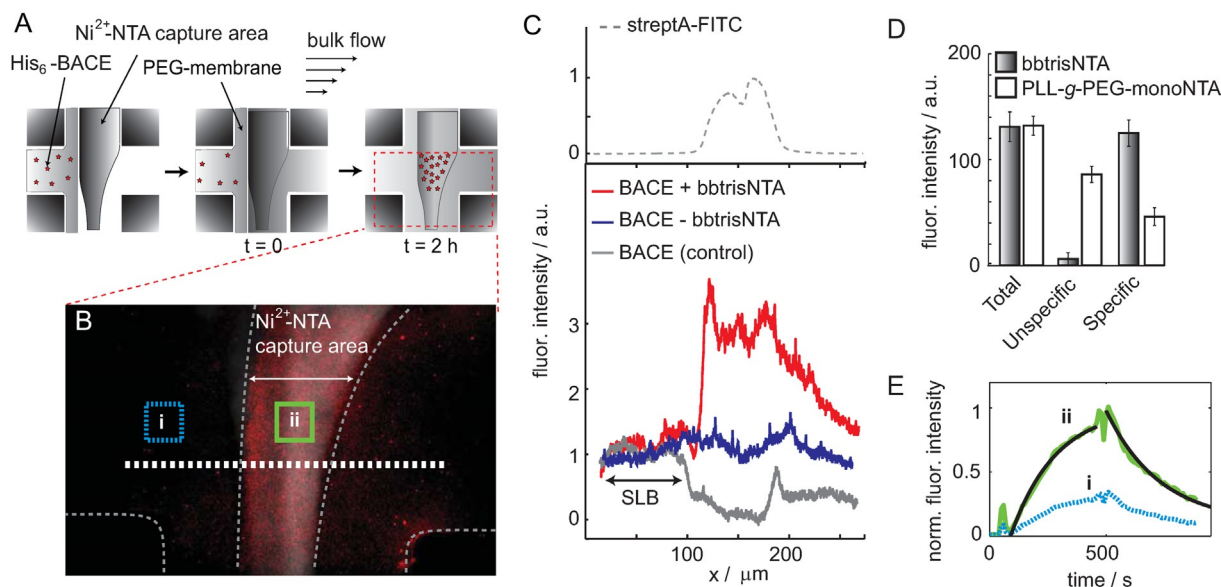
Figure 4. A) Schematic illustration of the affinity capture strategy. Bulk flow is started at $t = 0$. B) Fluorescence micrograph overlay ($270 \times 170 \ \mu m^2$) of Rho-PI bound to BACE (red) on adsorbed streptA-FITC-bbtrisNTA (grey). Contrast settings emphasize BACE accumulation at the functionalized stripe although the surrounding dark area contains baseline coverage of BACE (see intensity profiles). C) Intensity profile across channel (white dotted line in B) in the presence (red) and absence (blue) of bbtrisNTA-Ni^{2+}. As an additional control experiment, Rho-PI was added prior to protein movement (grey). Also shown is the corresponding profile for streptA-FITC (dotted line). D) Extracted fluorescence intensities above baseline of Rho-PI bound to BACE at bbtrisNTA (grey) and PLL-g-PEG-mono-NTA (white) stripe. Specific signal = total signal − unspecific signal (measured in the absence of NTA). E) Time-resolved binding trace of Rho-PI to membrane-embedded BACE at baseline density (i, blue square in micrograph) and accumulated density at stripe (ii, green square) with corresponding Langmuir model fit (black), which yield $k_{on} = 9 \times 10^3 \ M^{-1} s^{-1}$ and $k_{off} = 0.0043 \ s^{-1}$.

Flow-induced movement and capture of mobile BACE at the NTA-modified stripe, as verified by binding of Rho-PI (Figure 4B), resulted in a three-fold increase in protein accumulation (Figure 4C), demonstrating specific, affinity-based capture of a transmembrane protein embedded in a continuous (extending centimeters) lipid membrane. The absence of bbtrisNTA-Ni^{2+} resulted in a homogenous distribution of BACE close to the baseline coverage level, confirming specific capturing by using the conjugate (Figure 4C). To verify that the observed intensity stripe was not caused by unspecific binding of Rho-PI to exposed SiO$_2$ or to the bbtrisNTA-Ni^{2+}-modified stripe (e.g. because of a non-continuous SLB), Rho-PI was added prior to initiating the SLB motion, demonstrating binding exclusively to the BACE-containing SLB (Figures 4C and S6).

Corresponding experiments with PLL-g-PEG-mono-NTA-Ni^{2+} at the capturing area displayed a similar local increase in BACE coverage (Figures 4D and S5). However, a measurable BACE accumulation was observed also in the absence of NTA-Ni^{2+}, suggesting unspecific attractive interactions between BACE and PLL-g-PEG. Taking this nonspecific binding into account, specific BACE accumulation was approximately 30% of the accumulation to bbtrisNTA-Ni^{2+} (Figure 4D and S5), which likely reflects the weaker interaction of the mono-NTA compared to the better performing bbtrisNTA-Ni^{2+}.

The microfluidic setup, in combination with time-lapse imaging, enable time-resolved monitoring of ligand (Rho-PI) binding. Figure 4E illustrates such a kinetic trace, which can readily be fitted to a Langmuir binding model (black fit). Importantly, accumulation of BACE at the NTA-Ni^{2+} stripe (green square, Figure 4B ii) clearly enhances the signal-to-noise ratio, as com-pared to the reference SLB (blue square, Figure 4B i), demon-strating the value of surface enrichment of protein in ligand–receptor interaction studies.

To conclude, these proof-of-concept results show that trans-membrane, full-length proteins can be laterally manipulated, locally accumulated, and specifically captured in a stationary band while residing in a lipid membrane environment. The rel-atively modest accumulation may be significantly improved by, for example, covalent surface attachment of streptavidin, re-sulting in an increased surface density of NTA capture moieties. By using a fluorescently labeled substrate analogue inhibitor (Rho-PI), we demonstrated that BACE was able to bind sub-strate-like molecules in its active site after capture, which sug-gests that the enzyme retained both its structure and function. The advent of two-dimensional membrane protein affinity cap-turing in a lipid-bilayer environment may potentially be ex-panded from local capturing and enrichment of a single type of membrane protein to isolation of specific membrane pro-teins in a complex matrix, once the concept is extended to supported membranes derived directly from live cells. Parallel activities to address the challenge of converting cell-mem-brane material into a continuous SLBs are indeed ongoing.[31] If such efforts are successfully combined with the concept pre-sented herein, we believe that the approach may provide sev-eral new exciting opportunities for membrane protein analysis, such as identification of unknown membrane protein–protein or lipid–protein interactions as well as drug screening of mem-brane-embedded receptors including kinetic profiling facilitat-ed by the microfluidic setup.

[1] A. L. Hopkins, C. R. Groom, *Nat. Rev. Drug Discovery* **2002**, *1*, 727–730.

[2] A. M. Seddon, P. Curnow, P. J. Booth, *Biochim. Biophys. Acta Biomembr.* **2004**, *1666*, 105–117.

[3] J. L. Rigaud, D. Levy, *Methods Enzymol.* **2003**, *372*, 65–86.

[4] S. G. Patching, *Biochim. Biophys. Acta Biomembr.* **2014**, *1838*, 43–55.

[5] M. Stelzle, R. Miehlich, E. Sackmann, *Biophys. J.* **1992**, *63*, 1346–1354.

[6] C. Dietrich, R. Tampe, *Biochim. Biophys. Acta Biomembr.* **1995**, *1238*, 183–191.

[7] S. Daniel, A. J. Diaz, K. M. Martinez, B. J. Bench, F. Albertorio, P. S. Cremer, *J. Am. Chem. Soc.* **2007**, *129*, 8072–8073.

[8] C. Liu, C. F. Monson, T. Yang, H. Pace, P. S. Cremer, *Anal. Chem.* **2011**, *83*, 7876–7880.

[9] L. Kam, S. G. Boxer, *Langmuir* **2003**, *19*, 1624–1631.

[10] J. Neumann, M. Hennig, A. Wixforth, S. Manus, J. O. Radler, M. F. Schneider, *Nano Lett.* **2010**, *10*, 2903–2908.

[11] P. Jönsson, J. P. Beech, J. O. Tegenfeldt, F. Höök, *J. Am. Chem. Soc.* **2009**, *131*, 5294–5297.

[12] P. Jönsson, A. Gunnarsson, F. Höök, *Anal. Chem.* **2011**, *83*, 604–611.

[13] L. Simonsson, A. Gunnarsson, P. Wallin, P. Jonsson, F. Hook, *J. Am. Chem. Soc.* **2011**, *133*, 14027–14032.

[14] A. van Oudenaarden, S. G. Boxer, *Science* **1999**, *285*, 1046–1048.

[15] H. Nabika, A. Sasaki, B. Takimoto, Y. Sawai, S. He, K. Murakoshi, *J. Am. Chem. Soc.* **2005**, *127*, 16786–16787.

[16] T. Motegi, H. Nabika, K. Murakoshi, *Langmuir* **2012**, *28*, 6656–6661.

[17] J. T. Groves, C. Wulfing, S. G. Boxer, *Biophys. J.* **1996**, *71*, 2716–2723.

[18] S. J. Johnson, T. M. Bayerl, D. C. McDermott, G. W. Adam, A. R. Rennie, R. K. Thomas, E. Sackmann, *Biophys. J.* **1991**, *59*, 289–294.

[19] S. L. Cole, R. Vassar, *Curr. Alzheimer Res.* **2008**, *5*, 100–120.

[20] S. Sinha, J. P. Anderson, R. Barbour, G. S. Basi, R. Caccavello, D. Davis, M. Doan, H. F. Dovey, N. Frigon, J. Hong, K. Jacobson-Croak, N. Jewett, P. Keim, J. Knops, I. Lieberburg, M. Power, H. Tan, G. Tatsuno, J. Tung, D. Schenk, P. Seubert, S. M. Suomensaari, S. Wang, D. Walker, J. Zhao, L. McConlogue, V. John, *Nature* **1999**, *402*, 537–540.

[21] Y. Gambin, R. Lopez-Esparza, M. Reffay, E. Sierecki, N. S. Gov, M. Genest, R. S. Hodges, W. Urbach, *Proc. Natl. Acad. Sci. USA* **2006**, *103*, 2098–2102.

[22] M. Kühner, R. Tampé, E. Sackmann, *Biophys. J.* **1994**, *67*, 217–226.

[23] A. Graneli, C. C. Yeykal, R. B. Robertson, E. C. Greene, *Proc. Natl. Acad. Sci. USA* **2006**, *103*, 1221–1226.

[24] M. L. Wagner, L. K. Tamm, *Biophys. J.* **2000**, *79*, 1400–1414.

[25] E. Reimhult, M. Zach, F. Hook, B. Kasemo, *Langmuir* **2006**, *22*, 3313–3319.

[26] N. Huang, R. Michel, J. Voros, M. Textor, R. Hofer, A. Rossi, D. Elbert, J. Hubbell, N. Spencer, *Langmuir* **2001**, *17*, 489–498.

[27] G. Zhen, D. Falconnet, E. Kuennemann, J. Vörös, N. D. Spencer, M. Textor, S. Zürcher, *Adv. Funct. Mater.* **2006**, *16*, 243–251.

[28] D. J. Oshannessy, K. C. Odonnell, J. Martin, M. Brighamburke, *Anal. Biochem.* **1995**, *229*, 119–124.

[29] Z. Huang, P. Hwang, D. S. Watson, L. Cao, F. C. Szoka Jr., *Bioconjug. Chem.* **2009**, *20*, 1667–1672.

[30] S. Lata, A. Reichel, R. Brock, R. Tampe, J. Piehler, *J. Am. Chem. Soc.* **2005**, *127*, 10205–10215.

[31] H. Pace, L. Simonsson Nystrom, A. Gunnarsson, E. Eck, C. Monson, S. Geschwindner, A. Snijder, F. Hook, *Anal. Chem.* **2015**, *87*, 9194–9203.